

1 **Supplementary material for**

2 **High-Pressure Induced Guest-Mediated Gate Opening Behaviour of the**
3 **Co-Based Framework ZIF-67**

4

5 Isabelle M Jones,^{*a} Gemma F. Turner,^a Kari Pitts,^b Rees Powell,^b Alan Riboldi-Tunncliffe,^c Rachel Williamson,^c Stephanie
6 Boer,^c Lauren Allen^a and Stephen A. Moggach^{*a}

7

8 ^a. *School of Molecular Sciences, The University of Western Australia, 35 Stirling Highway, Crawley, WA 6009, Australia.*

9 ^b. *ChemCentre, Resources and Chemistry Precinct Level 2, South Wing, Building 500 Corner Manning Road and, Townsing
10 Dr, Bentley WA 6102*

11 ^c. *Australian Synchrotron, 800 Blackburn Road, Clayton, Victoria, Australia 3168*

12

13

14

15

16

17

18

19

20

21

22

23

24

25

26

27

28	Contents	
29	S1 Single crystal crystallography data	3
30	S2 Calculation of the Bulk Modulus.....	9
31	S3 Colour change in ZIF-67 in N₂.....	10
32	S4 UV-Vis spectroscopy of ZIF-67	10
33	SI References	11
34		
35		
36		

37 S1 Single crystal crystallography data

38 Synthesis of ZIF-67

39 Co(NO₃)₂·6H₂O (0.058 g, 2×10⁻⁴ mol) and 2-methylimidazole (MeIm; 0.016 g, 2×10⁻⁴ mol) were dissolved at 140°C in 4.5 mL
40 of *N,N'*-dimethylformamide (DMF) in a 12 mL capped borosilicate glass vial for 24h. The mixture was filtered, and the
41 resulting bright purple crystals were washed in ethanol three times at ambient temperature to facilitate exchange of the
42 DMF solvent and remove any unreacted linker. The sample was then dried under vacuum.

43 Laboratory Ambient Data Collection

44 An ambient pressure single-crystal structure of ZIF-67 (crystal 1) was collected using a Rigaku XtaLAB Synergy-S
45 diffractometer equipped with a Hypix-6000HE detector using Cu K α radiation ($\lambda = 1.54184 \text{ \AA}$). The sample was cooled using
46 a Cryostream operating at 100 K, and data were collected, integrated, and corrected for adsorption using CrysAlisPRO.¹ A
47 second crystal (crystal 2) was later collected at ambient temperature and pressure using Mo K α radiation ($\lambda = 0.7107 \text{ \AA}$),
48 and used to compare the ambient temperature volumes/bond lengths.

49 Laboratory High-Pressure LN₂ Data Collection

50 A ZIF-67 crystal (crystal 1) was loaded into a Merrill Bassett diamond anvil cell (DAC)² containing two Boehlar-Almax
51 diamond anvils with 600 μm culet faces fixed to tungsten-carbide backing discs.³ The DACs had a 40° half-opening angle. A
52 300 μm hole was drilled through a 200 μm thick tungsten gasket and fixed to one of the diamond culets to create a
53 cylindrical sample chamber. Ruby crystals were also loaded into the sample chamber and used as a pressure calibrant,
54 measured using the ruby fluorescence technique.⁴ Steel springs were placed around the guide pins on the DAC so that the
55 cell could be held open while submerged in liquid nitrogen (LN₂).⁵ The DAC was closed and placed in an LN₂ bath. The DAC
56 was allowed to equilibrate to a stable temperature (minimal bubbling) before being opened to a pre-determined height
57 and allowed to re-equilibrate. After bubbling had minimised, the DAC was closed and allowed to return to room
58 temperature before the pressure was measured. The ZIF-67 crystal was then compressed using the LN₂ as the pressure
59 transmitting medium (PTM), from 0.43 to 4.9 GPa in ~0.3 GPa intervals.

60 Diffraction data were collected on a Rigaku Oxford Diffraction XtaLAB Synergy-S at room temperature using Mo K α radiation
61 ($\lambda = 0.7107 \text{ \AA}$). A pre-experiment was used to determine the best data collection strategy in CrysAlis Pro¹, assuming a half-
62 opening angle of 40°. As above, a resolution cut-off to 1.11 \AA was applied initially and was gradually reduced to 1.00 \AA as the
63 gasket thinned. Adsorption was corrected using SADABS.⁶

64 Synchrotron High-Pressure Single Crystal Data Collection

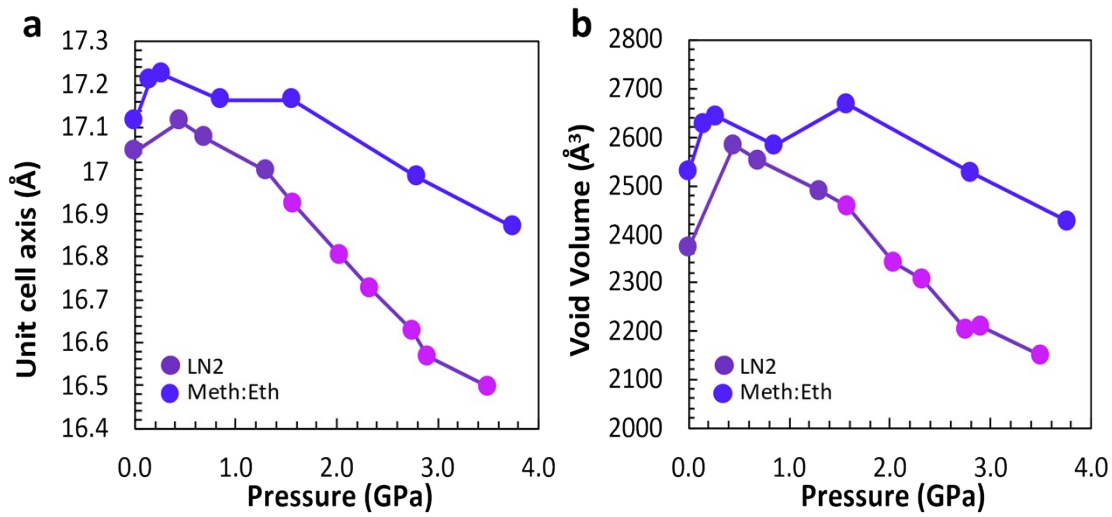
65 A single crystal of the as-prepared ZIF-67 was collected at the ANSTO (Australian Synchrotron) MX1 beamline in a modified
66 micro-Merrill Basset DAC, following the method of Boer et al.⁷ The crystal was first analysed at ambient pressure and
67 temperature. The crystal was then loaded into a micro-Merrill Basset DAC with a ruby chip as pressure calibrant, and a pre-
68 indented tungsten gasket fixed to the opposing diamond face. A 4:1 methanol/ethanol mixture (MeOH:EtOH) was used as
69 pressure-transmitting medium. The collected frames were unpacked using the EIGER HDF5 to miniCBF converter
70 (<https://github.com/biochem-fan/eiger2cbf>), and peaks were indexed and reduced using CrysAlisPro¹, with a 40° cut-off
71 mask. As above, a resolution cut-off to 1.11 \AA was applied initially and reduced to 0.9 \AA as the gasket thinned. SADABS⁶ was
72 used to correct for adsorption and checked through XPREP.⁸

73 Crystal Structure Refinements

74 The ambient pressure structures were solved using intrinsic phasing by SHELXT⁹ through the Olex2 1.5¹⁰ interface and
75 refined against $|F^2|$ using SHELXL.¹¹ These coordinates were used to refine all the high-pressure structures. At ambient
76 pressure, thermal similarity restraints were applied to all non-hydrogen atoms, hydrogens were constrained geometrically
77 to ride their host atoms, and all angles and bond distances were allowed to refine freely. High-pressure structures used the
78 ambient pressure atomic coordinates were used as starting positions and then refined against $|F^2|$ using SHELXL¹¹ within
79 Olex2.¹⁰

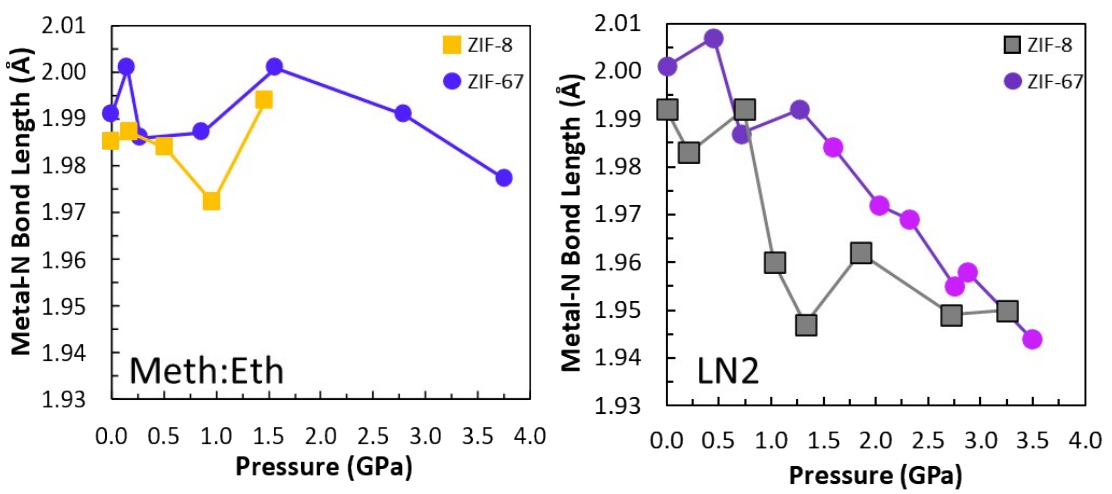
80 In structures under pressure, 1,2 and 1,3 distances were restrained to those found in the ambient structure, all metal-
81 nitrogen bonds were allowed to refine freely. H-atoms were placed geometrically and fixed to ride their host atoms.
82 Thermal similarity restraints were imposed for all C and N atoms in the ligand. In the LN₂ experiments, the location and
83 occupancy of N atoms within the pores were refined and compared to electron densities modelled using the Platon
84 SQUEEZE¹² algorithm.

85
86 The Crystallographic data reported and used in this paper have been deposited at the Cambridge Crystallographic Data Centre
87 repository under reference codes (2299159-2299176). Copies of the data can be obtained free of charge by visiting
88 <https://www.ccdc.cam.ac.uk/structures/>, or Cambridge Crystallographic Data Centre, 12 Union Road, Cambridge CB2 1EZ,
89 U.KCB21EZ, UK (fax +441223336033; deposit@ccdc.cam.ac.uk).



90
91
92
93

Figure S11: a) Length of the unit cell axes and b) void volume of ZIF-67 on compression in different PTM.



94
95
96
97
98
99

Figure S12: Length of the Metal-N bond of ZIF-8(Zn) and ZIF-67(Co) on compression in different PTM. ZIF-8 data was extracted from published crystallographic data for meth:eth¹³ and LN₂⁵ PTMs.

100 **Table S1.** Single Crystal crystallography data of ZIF-67 in 1:4 methanol:ethanol at the Australian Synchrotron (CCDC 2299169 – 2299175).

Pressure (GPa)	0.00	0.15	0.28	0.86	1.57	2.80	3.76
CCDC Deposition #	2299175	2299169	2299170	2299171	2299172	2299173	2299174
Chemical formula	C ₈ H ₁₀ CoN ₄ ·1.417[C ₂ H ₅ O H]	C ₈ H ₁₀ CoN ₄ ·3.167[CH ₃ O H]	C ₈ H ₁₀ CoN ₄ ·3.75[CH ₃ O H]	C ₈ H ₁₀ CoN ₄ ·3.833[CH ₃ O H]	C ₈ H ₁₀ CoN ₄ ·5.583[CH ₃ O H]	C ₈ H ₁₀ CoN ₄ ·4.5[CH ₃ OH]	C ₈ H ₁₀ CoN ₄ ·4.833[CH ₃ O H]
Crystal system, space group	Cubic, <i>I43m</i>	Cubic, <i>I43m</i>	Cubic, <i>I43m</i>	Cubic, <i>I43m</i>	Cubic, <i>I43m</i>	Cubic, <i>I43m</i>	Cubic, <i>I43m</i>
M_r	290.23	314.68	341.29	338.71	394.79	365.32	375.9
a (Å)	17.1155 (2)	17.2086 (4)	17.2230 (4)	17.1640 (3)	17.1651 (3)	16.9823 (4)	16.8677 (5)
v (Å³)	5013.82 (18)	5096.1 (4)	5108.9 (3)	5056.6 (3)	5057.5 (3)	4897.7 (4)	4799.2 (4)
μ (mm⁻¹)	1.02	1.02	1.02	1.03	1.05	1.08	1.1
Crystal size (mm)	0.15 × 0.1 × 0.1	0.15 × 0.1 × 0.1	0.15 × 0.1 × 0.1	0.15 × 0.1 × 0.1	0.15 × 0.1 × 0.1	0.15 × 0.1 × 0.1	0.15 × 0.1 × 0.1
Data collection							
Absorption correction	Multi-scan SADABS2016/2 (Bruker,2016/2) was used for absorption correction. wR2(int) was 0.1140 before and 0.0945 after correction. The Ratio of minimum to maximum transmission is 0.5854.	Multi-scan SADABS2016/2 (Bruker,2016/2) was used for absorption correction. wR2(int) was 0.0591 before and 0.0472 after correction. The Ratio of minimum to maximum transmission is 0.9342.	Multi-scan SADABS2016/2 (Bruker,2016/2) was used for absorption correction. wR2(int) was 0.1006 before and 0.0751 after correction. The Ratio of minimum to maximum transmission is 0.5921.	Multi-scan SADABS2016/2 (Bruker,2016/2) was used for absorption correction. wR2(int) was 0.1236 before and 0.0879 after correction. The Ratio of minimum to maximum transmission is 0.6922.	Multi-scan SADABS2016/2 (Bruker,2016/2) was used for absorption correction. wR2(int) was 0.1055 before and 0.0866 after correction. The Ratio of minimum to maximum transmission is 0.7704.	Multi-scan SADABS2016/2 (Bruker,2016/2) was used for absorption correction. wR2(int) was 0.0618 before and 0.0512 after correction. The Ratio of minimum to maximum transmission is 0.8714.	Multi-scan SADABS2016/2 (Bruker,2016/2) was used for absorption correction. wR2(int) was 0.0959 before and 0.0767 after correction. The Ratio of minimum to maximum transmission is 0.7437.
T_{min} T_{max}	0.436, 0.744	0.696, 0.745	0.441, 0.745	0.516, 0.745	0.574, 0.745	0.649, 0.745	0.554, 0.745
No. of measured, independent and observed [I > 2σ(I)] reflections	1193, 348, 327	2148, 515, 507	2030, 531, 495	1912, 638, 566	2236, 627, 581	2324, 632, 624	2322, 623, 616
R_{int}	0.05	0.024	0.041	0.051	0.052	0.04	0.023
ϑ_{max} (°)	18.6	21.2	21.7	23.2	23.2	23.2	23.2
(sin ϑ/λ)_{max} (Å⁻¹)	0.449	0.508	0.519	0.554	0.554	0.554	0.555

104 **Table S1. continued** Single Crystal crystallography data of ZIF-67 in 1:4 methanol:ethanol at the Australian Synchrotron (CCDC 2299169 – 2299175).

Refinement							
$R[F^2 > 2\sigma(F^2)], wR(F^2), S$	0.029, 0.075, 1.08	0.018, 0.051, 1.12	0.043, 0.127, 1.20	0.083, 0.239, 1.11	0.061, 0.180, 1.13	0.037, 0.112, 1.20	0.028, 0.078, 1.10
No. of reflections	348	515	531	638	627	632	623
No. of parameters	24	24	24	25	24	24	23
No. of restraints	1	8	8	8	8	8	8
	$w = 1/[\sigma^2(F_o^2) + (0.008P)^2 + 0.4507P]$ where $P = (F_o^2 + 2F_c^2)/3$	$w = 1/[\sigma^2(F_o^2) + (0.0361P)^2 + 2.6871P]$ where $P = (F_o^2 + 2F_c^2)/3$	$w = 1/[\sigma^2(F_o^2) + (0.0419P)^2 + 7.1678P]$ where $P = (F_o^2 + 2F_c^2)/3$	$w = 1/[\sigma^2(F_o^2) + (0.1712P)^2 + 3.1104P]$ where $P = (F_o^2 + 2F_c^2)/3$	$w = 1/[\sigma^2(F_o^2) + (0.0731P)^2 + 15.2702P]$ where $P = (F_o^2 + 2F_c^2)/3$	$w = 1/[\sigma^2(F_o^2) + (0.0492P)^2 + 2.5349P]$ where $P = (F_o^2 + 2F_c^2)/3$	$w = 1/[\sigma^2(F_o^2) + (0.0254P)^2 + 2.7463P]$ where $P = (F_o^2 + 2F_c^2)/3$
$\Delta\rho_{max} \Delta\rho_{min}$ ($e \text{ \AA}^{-3}$)	0.10, -0.14	0.13, -0.11	0.26, -0.28	0.36, -0.59	0.44, -0.41	0.28, -0.33	0.18, -0.23
Absolute structure	Flack x determined using 124 quotients [(I+)-(I-)]/[(I+)+(I-)] (Parsons, Flack and Wagner, Acta Cryst. B69 (2013) 249-259).	Flack x determined using 203 quotients [(I+)-(I-)]/[(I+)+(I-)] (Parsons, Flack and Wagner, Acta Cryst. B69 (2013) 249-259).	Flack x determined using 179 quotients [(I+)-(I-)]/[(I+)+(I-)] (Parsons, Flack and Wagner, Acta Cryst. B69 (2013) 249-259).	Flack x determined using 210 quotients [(I+)-(I-)]/[(I+)+(I-)] (Parsons, Flack and Wagner, Acta Cryst. B69 (2013) 249-259).	Flack x determined using 220 quotients [(I+)-(I-)]/[(I+)+(I-)] (Parsons, Flack and Wagner, Acta Cryst. B69 (2013) 249-259).	Flack x determined using 258 quotients [(I+)-(I-)]/[(I+)+(I-)] (Parsons, Flack and Wagner, Acta Cryst. B69 (2013) 249-259).	Flack x determined using 250 quotients [(I+)-(I-)]/[(I+)+(I-)] (Parsons, Flack and Wagner, Acta Cryst. B69 (2013) 249-259).
Absolute structure parameter	0.11 (5)	0.114 (16)	0.14 (3)	0.27 (3)	0.22 (3)	0.14 (2)	0.124 (19)

105

106 **Table S2.** Single Crystal crystallography data of ZIF-67 in Nitrogen (CCDC 2299159 – 2299168, 2299176).

	Crystal 1*	Crystal 2									
Pressure	0	0.0[^]	0.45	0.71	1.27	1.59	2.03	2.32	2.75	2.88	3.49
CCDC Deposition #	2299160	2299176	2299159	2299168	2299161	2299162	2299163	2299164	2299165	2299166	2299167
Chemical formula	C ₈ H ₁₀ CoN ₄ ·1[CH ₂ CH ₃ OH]	C ₈ H ₁₀ CoN ₄ ·1.833[CH ₂ CH ₃ OH]	C ₈ H ₁₀ CoN ₄ ·0.646(N ₈)·0.167[CH ₂ CH ₃ OH]	C ₈ H ₁₀ CoN ₄ ·1.521(N ₄)	C ₈ H ₁₀ CoN ₄ ·12.889(N _{0.5})	C ₈ H ₁₀ CoN ₄ ·1.8(N _{0.5})	C ₈ H ₁₀ CoN ₄ ·2.433(N ₄)	C ₈ H ₁₀ CoN ₄ ·2.458(N ₄)	C ₈ H ₁₀ CoN ₄ ·1.8667(N _{0.5})	C ₈ H ₁₀ CoN ₄ ·1.8667(N _{0.5})	C ₈ H ₁₀ CoN ₄ ·1.8667(N _{0.5})
M_r	271.02	305.57	301.33	306.36	311.41	347.22	357.49	358.89	351.89	351.89	351.89
Temperature (K)	293	100	293	293	293	293	293	293	293	293	293
a (Å)	17.0441 (4)	16.9230 (5)	17.1155 (7)	17.0740 (4)	16.9979 (6)	16.9247 (6)	16.8057 (4)	16.7265 (4)	16.6284 (4)	16.5684 (3)	16.4992 (4)
V (Å³)	4951.3 (3)	4846.5 (4)	5013.8 (6)	4977.4 (3)	4911.2 (5)	4848.0 (5)	4746.5 (3)	4679.7 (3)	4597.8 (3)	4548.2 (2)	4491.4 (4)
Radiation type	Mo Kα	Cu Kα	Mo Kα	Mo Kα	Mo Kα	Mo Kα	Mo Kα	Mo Kα	Mo Kα	Mo Kα	Mo Kα
μ (mm⁻¹)	1.03	8.35	1.03	1.04	1.05	1.08	1.11	1.12	1.14	1.15	1.17
Crystal size (mm)	0.15 × 0.1 × 0.07	0.14 × 0.1 × 0.09	0.14 × 0.1 × 0.09	0.14 × 0.1 × 0.09	0.14 × 0.1 × 0.09	0.14 × 0.1 × 0.09	0.14 × 0.1 × 0.09	0.14 × 0.1 × 0.09	0.14 × 0.1 × 0.09	0.14 × 0.1 × 0.09	0.14 × 0.1 × 0.09
Data collection											
T_{min}, T_{max}	0.868, 1.000	0.475, 0.711	0.480, 0.744	0.440, 0.745	0.480, 0.745	0.516, 0.745	0.635, 0.706	0.628, 0.745	0.634, 0.745	0.676, 0.731	0.605, 0.745
No. of measured, independent and observed [I > 2σ(I)] reflections	6615, 888, 682	4186, 880, 741	3880, 366, 342	4014, 391, 373	5119, 505, 463	5113, 501, 460	9257, 496, 455	11050, 491, 458	7482, 409, 371	16850, 373, 346	7385, 470, 409
R_{int}	0.043	0.043	0.077	0.083	0.091	0.094	0.076	0.086	0.074	0.067	0.092
(sin θ/λ)_{max} (Å⁻¹)	0.625	0.628	0.443	0.452	0.499	0.5	0.5	0.500	0.554	0.458	0.500
Absorption correction	<i>Gaussian</i> CrysAlis PRO 1.171.41.115a (Rigaku Oxford Diffraction, 2021) Numerical absorption correction based on gaussian integration over a multifaceted crystal model Empirical absorption correction using spherical harmonics, implemented in SCALE3 ABSPACK scaling algorithm.	<i>Gaussian</i> CrysAlis PRO 1.171.42.58a (Rigaku Oxford Diffraction, 2022) Numerical absorption correction based on gaussian integration over a multifaceted crystal model Empirical absorption correction using spherical harmonics, implemented in SCALE3 ABSPACK algorithm.	<i>Multi-scan</i> SADABS2016/ 2 (Bruker,2016/ 2) was used for absorption correction. wR2(int) was 0.1072 before and 0.0718 after correction. The Ratio of minimum to maximum transmission is 0.6455. The λ/2 correction factor is Not present.	<i>Multi-scan</i> SADABS2016/ 2 (Bruker,2016/ 2) was used for absorption correction. wR2(int) was 0.1171 before and 0.0857 after correction. The Ratio of minimum to maximum transmission is 0.5910. The λ/2 correction factor is Not present.	<i>Multi-scan</i> SADABS2016/ 2 (Bruker,2016/ 2) was used for absorption correction. wR2(int) was 0.1078 before and 0.0816 after correction. The Ratio of minimum to maximum transmission is 0.6446. The λ/2 correction factor is Not present.	<i>Multi-scan</i> SADABS2016/ 2 (Bruker,2016/ 2) was used for absorption correction. wR2(int) was 0.1139 before and 0.0835 after correction. The Ratio of minimum to maximum transmission is 0.6928. The λ/2 correction factor is Not present.	<i>Multi-scan</i> SADABS2016/ 2 (Bruker,2016/ 2) was used for absorption correction. wR2(int) was 0.0984 before and 0.0867 after correction. The Ratio of minimum to maximum transmission is 0.8994. The λ/2 correction factor is Not present.	<i>Multi-scan</i> SADABS2016/ 2 (Bruker,2016/ 2) was used for absorption correction. wR2(int) was 0.1012 before and 0.0855 after correction. The Ratio of minimum to maximum transmission is 0.8439. The λ/2 correction factor is Not present.	<i>Multi-scan</i> SADABS2016/ 2 (Bruker,2016/ 2) was used for absorption correction. wR2(int) was 0.0907 before and 0.0782 after correction. The Ratio of minimum to maximum transmission is 0.8509. The λ/2 correction factor is Not present.	<i>Multi-scan</i> SADABS2016/ 2 (Bruker,2016/ 2) was used for absorption correction. wR2(int) was 0.0861 before and 0.0728 after correction. The Ratio of minimum to maximum transmission is 0.9243. The λ/2 correction factor is Not present.	<i>Multi-scan</i> SADABS2016/ 2 (Bruker,2016/ /2) was used for absorption correction. wR2(int) was 0.1018 before and 0.0855 after correction. The Ratio of minimum to maximum transmission is 0.8122. The λ/2 correction factor is Not present.

107 **Table S2. continued** Single Crystal crystallography data of ZIF-67 in Nitrogen (CCDC 2299159 – 2299168, 2299176).

Refinement											
$R[F^2 > 2\sigma(F^2)], wR(F^2), S$	0.035, 0.084, 0.95	0.057, 0.186, 1.09	0.066, 0.188, 1.19	0.067, 0.210, 1.25	0.080, 0.240, 1.13	0.082, 0.214, 1.11	0.072, 0.195, 1.11	0.074, 0.194, 1.16	0.087, 0.222, 1.18	0.080, 0.212, 1.15	0.085, 0.232, 1.14
No. of reflections	888	880	367	391	505	501	496	491	619	373	470
No. of parameters	24	24	38	47	43	45	48	49	54	54	54
No. of restraints	4	4	5	8	8	10	10	10	11	11	11
	$w = 1/[\sigma^2(F_o^2) + (0.0596P)^2]$ where $P = (F_o^2 + 2F_c^2)/33$	$w = 1/[\sigma^2(F_o^2) + (0.1222P)^2 + 1.1651P]$ where $P = (F_o^2 + 2F_c^2)/3$	$w = 1/[\sigma^2(F_o^2) + (0.1359P)^2 + 7.6237P]$ where $P = (F_o^2 + 2F_c^2)/3$	$w = 1/[\sigma^2(F_o^2) + (0.1469P)^2 + 11.7616P]$ where $P = (F_o^2 + 2F_c^2)/3$	$w = 1/[\sigma^2(F_o^2) + (0.1926P)^2]$ where $P = (F_o^2 + 2F_c^2)/3$	$w = 1/[\sigma^2(F_o^2) + (0.1666P)^2]$ where $P = (F_o^2 + 2F_c^2)/3$	$w = 1/[\sigma^2(F_o^2) + (0.1592P)^2 + 0.3076P]$ where $P = (F_o^2 + 2F_c^2)/3$	$w = 1/[\sigma^2(F_o^2) + (0.1547P)^2 + 0.2984P]$ where $P = (F_o^2 + 2F_c^2)/3$	$w = 1/[\sigma^2(F_o^2) + (0.1508P)^2]$ where $P = (F_o^2 + 2F_c^2)/3$	$w = 1/[\sigma^2(F_o^2) + (0.1472P)^2]$ where $P = (F_o^2 + 2F_c^2)/3$	$w = 1/[\sigma^2(F_o^2) + (0.1304P)^2 + 11.9372P]$ where $P = (F_o^2 + 2F_c^2)/3$
$\Delta\rho_{max} \Delta\rho_{min} (e \text{ \AA}^{-3})$	0.15, -0.18	0.30, -0.25	0.51, -0.40	0.62, -0.53	0.83, -0.38	0.73, -0.83	0.79, -0.68	0.90, -0.72	0.85, -0.81	0.75, -0.83	0.83, -0.79
Absolute structure	Flack x determined using 243 quotients [(+)-(-)]/[(+)+(-)] (Parsons, Flack and Wagner, Acta Cryst. B69 (2013) 249-259).	Flack x determined using 244 quotients [(+)-(-)]/[(+)+(-)] (Parsons, Flack and Wagner, Acta Cryst. B69 (2013) 249-259).	Flack x determined using 138 quotients [(+)-(-)]/[(+)+(-)] (Parsons, Flack and Wagner, Acta Cryst. B69 (2013) 249-259).	Flack x determined using 153 quotients [(+)-(-)]/[(+)+(-)] (Parsons, Flack and Wagner, Acta Cryst. B69 (2013) 249-259).	Flack x determined using 182 quotients [(+)-(-)]/[(+)+(-)] (Parsons, Flack and Wagner, Acta Cryst. B69 (2013) 249-259).	Flack x determined using 172 quotients [(+)-(-)]/[(+)+(-)] (Parsons, Flack and Wagner, Acta Cryst. B69 (2013) 249-259).	Flack x determined using 181 quotients [(+)-(-)]/[(+)+(-)] (Parsons, Flack and Wagner, Acta Cryst. B69 (2013) 249-259).	Flack x determined using 192 quotients [(+)-(-)]/[(+)+(-)] (Parsons, Flack and Wagner, Acta Cryst. B69 (2013) 249-259).	Flack x determined using 180 quotients [(+)-(-)]/[(+)+(-)] (Parsons, Flack and Wagner, Acta Cryst. B69 (2013) 249-259).	Flack x determined using 143 quotients [(+)-(-)]/[(+)+(-)] (Parsons, Flack and Wagner, Acta Cryst. B69 (2013) 249-259).	Flack x determined using 158 quotients [(+)-(-)]/[(+)+(-)] (Parsons, Flack and Wagner, Acta Cryst. B69 (2013) 249-259).
AS parameter	-0.033 (13)	-0.021 (11)	0.09 (4)	0.07 (3)	0.13 (3)	0.08 (3)	0.02 (2)	0.06 (2)	0.07 (2)	0.088 (18)	0.09 (2)

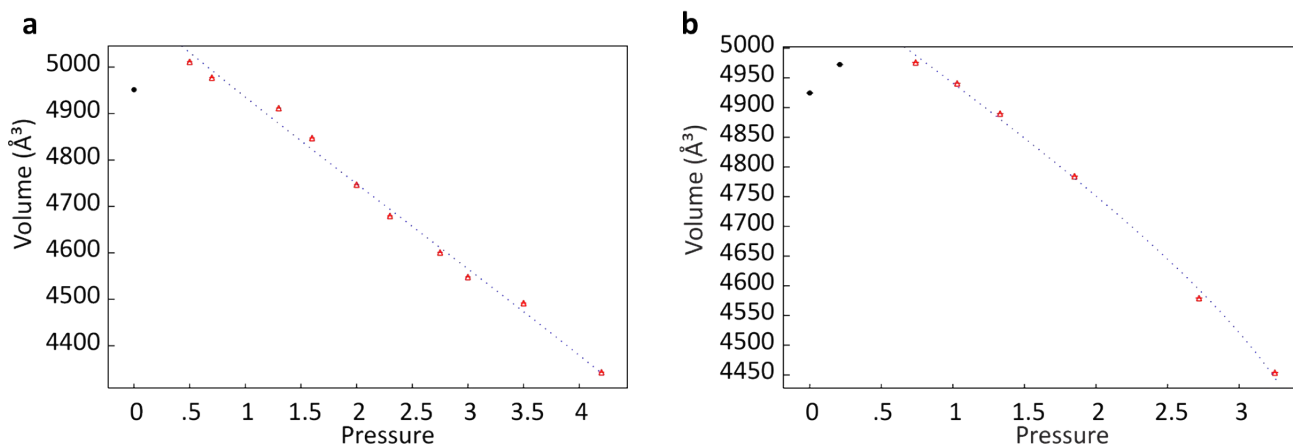
108

109 S2 Calculation of the Bulk Modulus

110 EoSFit7¹⁴ was used to fit the unit cell volume compression to a third-order Birch-Murnaghan equation of state to estimate the bulk
 111 modulus after the phase transition of ZIF-67 and ZIF-8 in LN2 (Figure S1). Pressure (P) is calculated in the equation below where V₀
 112 is the volume at ambient pressure, V is the volume at any given pressure, K₀ is the isothermal bulk modulus, and K' is the pressure
 113 derivative of the isothermal bulk modulus.

$$P = \frac{3K_0}{2} \left[\left(\frac{V}{V_0} \right)^{\frac{7}{3}} - \left(\frac{V}{V_0} \right)^{\frac{5}{3}} \right] + \left[1 + \frac{1}{3} (K'_{T_0} - 4) \left\{ \left(\frac{V}{V_0} \right)^{\frac{2}{3}} - 1 \right\} \right] \quad (1)$$

114
 115

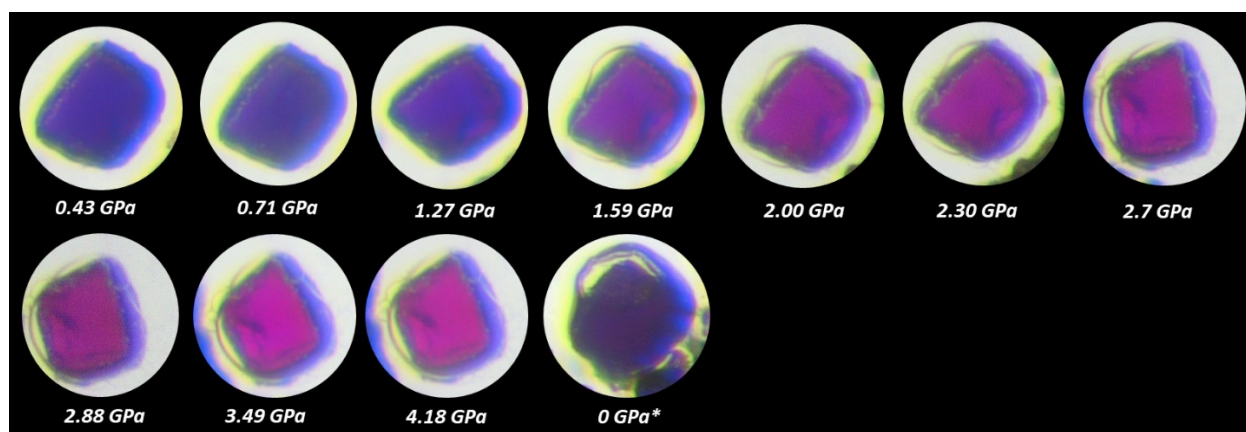


116

117 **Figure S13:** Fits of the third-order Birch-Murnaghan (solid lines) to the unit cell volume of (a) ZIF-8 and (b) ZIF-67 during compression
 118 using N2 as the PTM, as determined by EoSFit7.¹⁴

119

120 S3 Colour change in ZIF-67 in N₂



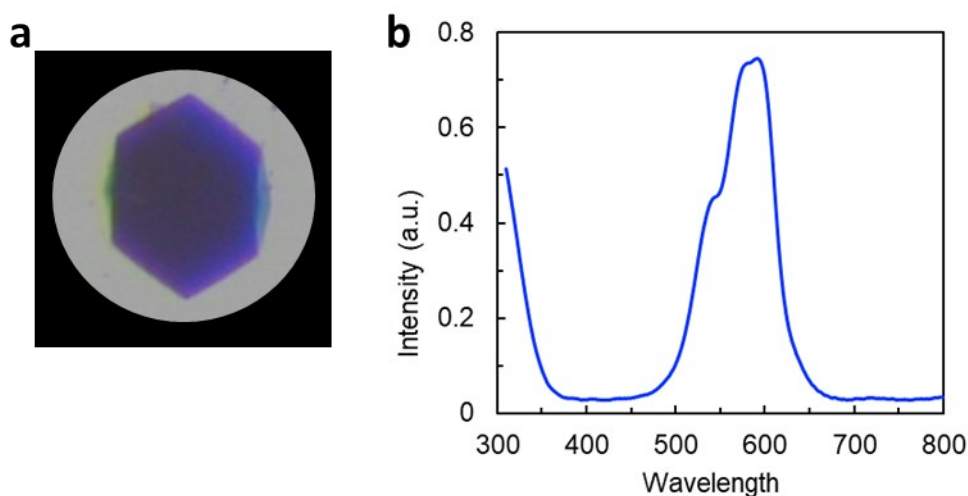
121
122 **Figure S14:** Colour change in the ZIF-67 crystal in LN₂ with increasing pressure. Micrographs were taken at the same magnification
123 and using the same back and forward light settings. The final micrograph (0 GPa*) shows the crystal after release of pressure, showing
124 the almost complete reversal of the colour transition, although the crystal does appear less blue than typical ambient crystals.

125

126 S4 UV-Vis spectroscopy of ZIF-67

127 A single crystal of ZIF-67 was crushed on a quartz glass slide using one half of a micro-diamond compression cell. The UV-Vis colour
128 absorbance spectrum of the crystal was measured in transmission orientation mode at wavelengths between 310–800nm at
129 ~0.436nm resolution using a Craic 20/30PV Microspectrophotometer. Each scan was collected using a 15x objective lens, and an
130 aperture of 19.6 x 19.6 microns. The spectra comprise 100 scans, for a total acquisition time of 14ms, that are background corrected
131 against blank air/diamond collected prior to sample spectra acquisition. NIST traceable holmium oxide and didymium standards were
132 used to calibrate wavelength accuracy. Photometric accuracy was calibrated using three neutral density standards.

133



134
135 **Figure S15:** a) a typical crystal of ZIF-67 and b) the UV-Vis spectrum of a single ZIF-67 crystal.

136

137 SI References

- 138 1 Rigaku Oxford Diffraction, CrysAlisPro Software System, *Rigaku Corporation, Oxford, UK*, 2023.
139 2 L. Merrill and W. A. Bassett, *Rev Sci Instrum*, 1974, **45**, 290. DOI: 10.1063/1.1686607
140 3 S. A. Moggach, D. R. Allan, S. Parsons and J. E. Warren, *J Appl Crystallogr*, 2008, **41**, 249–251. DOI: 10.1107/S0021889808000514
141 4 G. J. Piermarini, S. Block, J. D. Barnett, and R. A. Forman, *J Appl Phys*, 1975, **46**, 2774–2780. DOI: 10.1063/1.321957
142 5 C. L. Hobday, C. H. Woodall, M. J. Lennox, M. Frost, K. Kamenev, T. Düren, C. A. Morrison and S. A. Moggach, *Nat Commun*, 2018, **9**, 1–9. DOI:
143 10.1038/s41467-018-03878-6
144 6 G. M. Sheldrick, SADABS, Program for area detector adsorption correction, *University of Göttingen, Germany*, 1996.
145 7 S. A. Boer, J. R. Price, A. Riboldi-Tunncliffe, R. Williamson, A. Summers, G. F. Turner, I. Jones, C. Bond, A. Vrielink, A. C. Marshall, J. Hitchings and S.
146 A. Moggach, *J Synchrotron Radiat*, 2023, **30**, 841–846. DOI: 10.1107/S160057752300406
147 8 Bruker AXS Inc, APEX2, XPREP and SAINT, *Madison, Wisconsin, USA*, 2007.
148 9 G. M. Sheldrick and IUCr, *Acta Crystallogr A Found Adv*, 2015, **71**, 3–8. DOI: 10.1107/S2053273314026370
149 10 O. V. Dolomanov, L. J. Bourhis, R. J. Gildea, J. A. K. Howard and H. Puschmann, *J Appl Crystallogr*, 2009, **42**, 339–341. DOI:
150 10.1107/S0021889808042726
151 11 G. M. Sheldrick, *Acta Crystallogr C Struct Chem*, 2015, **71**, 3–8. DOI: 10.1107/S2053229614024218
152 12 A. L. Spek, *Acta Crystallogr C Struct Chem*, 2015, **71**, 9–18. DOI: 10.1107/S2053229614024929
153 13 S. A. Moggach, T. D. Bennett and A. K. Cheetham, *Angewandte Chemie Int Ed*, 2009, **48**, 7087–7089. DOI: 10.1002/anie.200902643
154 14 J. Gonzalez-Platas, M. Alvaro, F. Nestola and R. Angel, *J Appl Crystallogr*, 2016, **49**, 1377–1382. DOI: 10.1107/S1600576716008050